







RESEARCH ARTICLE | SEPTEMBER 10 2020

## Ultrafast excited state dynamics of silver ion-mediated cytosine–cytosine base pairs in metallo-DNA

Special Collection: [65 Years of Electron Transfer](#)

Forrest R. Kohl   ; Yuyuan Zhang; Aaron P. Charnay; Lara Martínez-Fernández   ; Bern Kohler  



*J. Chem. Phys.* 153, 105104 (2020)

<https://doi.org/10.1063/5.0020463>

 CHORUS



View  
Online



Export  
Citation

[CrossMark](#)

# Ultrafast excited state dynamics of silver ion-mediated cytosine–cytosine base pairs in metallo-DNA

Cite as: J. Chem. Phys. 153, 105104 (2020); doi: 10.1063/5.0020463

Submitted: 30 June 2020 • Accepted: 17 August 2020 •

Published Online: 10 September 2020



Forrest R. Kohl,<sup>1</sup>  Yuyuan Zhang,<sup>1</sup> Aaron P. Charnay,<sup>1</sup> Lara Martínez-Fernández,<sup>2,a)</sup>  and Bern Kohler<sup>1,a)</sup> 

## AFFILIATIONS

<sup>1</sup>Department of Chemistry and Biochemistry, 100 W. 18th Ave., Columbus, Ohio 43210, USA

<sup>2</sup>Departamento de Química, Facultad de Ciencias and Institute for Advanced Research in Chemistry (IADCHEM), Universidad Autónoma de Madrid, Campus de Excelencia UAM-CSIC, Cantoblanco, 28049 Madrid, Spain

**Note:** This paper is part of the JCP Special Topic on 65 Years of Electron Transfer.

**a)** Authors to whom correspondence should be addressed: [lara.martinez@uam.es](mailto:lara.martinez@uam.es) and [kohler.40@osu.edu](mailto:kohler.40@osu.edu)

## ABSTRACT

To better understand the nexus between structure and photophysics in metallo-DNA assemblies, the parallel-stranded duplex formed by the all-cytosine oligonucleotide, dC<sub>20</sub>, and silver nitrate was studied by circular dichroism (CD), femtosecond transient absorption spectroscopy, and time-dependent-density functional theory calculations. Silver(I) ions mediate Cytosine–Cytosine (CC) base pairs by coordinating to the N3 atoms of two cytosines. Although these silver(I) mediated CC base pairs resemble the proton-mediated CC base pairs found in i-motif DNA at first glance, a comparison of experimental and calculated CD spectra reveals that silver ion-mediated i-motif structures do not form. Instead, the parallel-stranded duplex formed between dC<sub>20</sub> and silver ions is proposed to contain consecutive silver-mediated base pairs with high propeller twist-like ones seen in a recent crystal structure of an emissive, DNA-templated silver cluster. Femtosecond transient absorption measurements with broadband probing from the near UV to the near IR reveal an unusually long-lived (>10 ns) excited state in the dC<sub>20</sub> silver ion complex that is not seen in dC<sub>20</sub> in single-stranded or i-motif forms. This state is also absent in a concentrated solution of cytosine–silver ion complexes that are thought to assemble into planar ribbons or sheets that lack stacked silver(I) mediated CC base pairs. The large propeller twist angle present in metal-mediated base pairs may promote the formation of long-lived charged separated or triplet states in this metallo-DNA.

Published under license by AIP Publishing. <https://doi.org/10.1063/5.0020463>

## I. INTRODUCTION

In DNA strands, the spatial organization of nucleobases profoundly affects the dynamics of excited states formed by UV light.<sup>1,2</sup> Excited states of stacked bases, both in single and double strands, frequently decay on much slower timescales than excited states of nucleobase monomers. These long-lived excited states have the character of radical pairs and form in <1 ps from charge transfer (CT) excited states that most often involve two stacked bases on the same strand.<sup>3,4</sup> As would be expected from their high degree of charge transfer character, Marcus theory can successfully correlate the decay rates of these states with the driving force for back electron transfer or charge recombination.<sup>5</sup>

Experiments reported to date show that the lifetimes of typical DNA CT excited states, which lie in the range of tens to hundreds of ps, are rather insensitive to DNA strand conformation apart from the key requirement that the bases are stacked at the instant of excitation. For example, excited state deactivation has been shown to proceed nearly unchanged for excited states in the B and Z forms of the d(GC)<sub>9</sub>-d(GC)<sub>9</sub> duplex,<sup>6</sup> and, in a series of single-stranded diadenosines with backbone modifications, common excited state lifetimes were observed even when the helical twist angle was changed or when one base was flipped to stack with its opposite face.<sup>7</sup> These results disclose a need for additional study of excited state dynamics in DNA strands, particularly in ones with unusual conformations.

DNA nucleobases bind a variety of metal ions, and the resulting metal-mediated base pairs greatly expand the structural repertoire of DNA.<sup>8,9</sup> These “metallo-DNA”<sup>10</sup> systems are of interest because the metal ions do not just manipulate and direct the three-dimensional structure, but they also confer novel electronic properties as a result of nucleobase–metal ion interactions. Snyder *et al.*<sup>11</sup> recently showed that self-assembled structures formed by Ag<sup>+</sup> ions and adenine have long-lived excited states that are very similar to the ones seen in DNA strands with stacked adenines. In this case, the metal ions appear to template base stacked structures that may be similar to the ones found in natural DNA strands, but the precise structures are currently unknown.

To better understand how metal ion binding affects the UV excited states of DNA strands, we report here on the excited state dynamics of dC<sub>20</sub> complexed with Ag<sup>+</sup> ions. Several factors motivate our interest in this system. First, this sequence can form a biologically significant intercalated structure by proton-mediated Cytosine–Cytosine (CC) base pairing (i-motif),<sup>12,13</sup> and there has been interest in whether similar structures form with Ag<sup>+</sup> ions.<sup>14,15</sup> Second, the excited-state dynamics of uncomplexed dC<sub>n</sub> sequences have been studied extensively by ultrafast spectroscopy,<sup>16–19</sup> revealing rich dynamics involving localized <sup>1</sup>nπ\* excited states and longer-lived excited states attributed to charge transfer from C to CH<sup>+</sup> in the i-motif structure. Third, dC<sub>n</sub><sup>20</sup> and other C-rich DNA sequences are important templates for forming fluorescent silver clusters. Fourth, and perhaps most importantly for this study, recently solved crystal structures for a variety of DNA strands and nucleobase monomers containing silver ion-mediated CC base pairs<sup>10,21–24</sup> provide key structural insights that can guide the interpretation of the effects of the nucleic acid secondary structure on the UV excited states.

The basic structural element that allows dC<sub>n</sub> sequences to form higher-order structures is the CC base pair mediated either by a silver ion or a proton. A single Ag<sup>+</sup> ion can bind to the N3 atoms of two cytosines (Cyt), forming a silver ion-mediated CC base pair, C–Ag<sup>+</sup>–C, in *trans* [Fig. 1(a)] or *cis* [Fig. 1(b)] geometry (*trans/cis* refers to the configuration of the glycosidic bonds about the N3–N3' axis). The *cis* C–Ag<sup>+</sup>–C base pair has been seen in crystal structures of antiparallel DNA duplexes containing one or more non-contiguous C–Ag<sup>+</sup>–C base pairs.<sup>25</sup>

The proton-mediated (also known as hemi-protonated) CC base pair, CH<sup>+</sup>–C, with three hydrogen bonds requires the *trans*

configuration [Fig. 1(c)] and is the basic building block of i-motif structures [a representative intramolecular i-motif is illustrated in Fig. 1(d)] adopted by many cytosine-rich sequences.<sup>13</sup> In the i-motif, a second pair of parallel strands, oriented antiparallel with respect to the first, allows CH<sup>+</sup>–C base pairs to intercalate or interdigitate such that the face of the nucleobase in each *trans* base pair (and, hence, the strand direction) alternates from one base pair to the next [Fig. 1(d), black and white squares]. The i-motif structure is generally favored at pH ~5, but a growing number of reports provide evidence of its formation at neutral pH,<sup>26</sup> and i-motifs have recently been detected in human cell nuclei.<sup>27</sup> The rigid character and pH responsiveness of the i-motif structure have also made its structure of great interest for DNA nanotechnology.<sup>28–30</sup>

Inspired by the ability of H<sup>+</sup> to mediate the i-motif structure (H-i-motif), and in light of the similar coordination of the Ag<sup>+</sup> ion with the N3 atoms of a pair of cytosine bases [Figs. 1(a)–1(c)], several authors discussed the possibility that Ag<sup>+</sup> ion complexation can result in an i-motif-like structure (Ag-i-motif).<sup>14,15,31</sup> However, Gwinn and co-workers presented convincing evidence from FRET and other experiments that dC<sub>n</sub> strands strictly associate as parallel-stranded duplexes in the presence of Ag<sup>+</sup> ions.<sup>29</sup> The different topology of a parallel duplex [Fig. 1(e)] compared to that of an i-motif structure [Fig. 1(d)] suggests that these structures should differ in their excited-state dynamics, motivating the present study.

Here, we use UV pump/broadband UV–visible (UV–vis)–near infrared (NIR) probe transient absorption (TA) spectroscopy to investigate the excited state dynamics of a cytosine homooligonucleotide (dC<sub>20</sub>) in the presence of silver(I) ions (Ag–dC<sub>20</sub>) in aqueous solution for the first time. These results are compared with measurements on the single strand (ss-dC<sub>20</sub>) and proton i-motif formed by the same sequence (i-dC<sub>20</sub>) to learn how base stacking and other underlying structural motifs influence excited state deactivation. We observe a very long-lived (>10 ns) state in Ag–dC<sub>20</sub> that is not seen in any of the other systems. The measured and calculated circular dichroism (CD) spectra show that Ag–dC<sub>20</sub> forms a right-handed double helical, parallel-duplex structure of stacked C–Ag<sup>+</sup>–C base pairs, each of which has high propeller twist. We suggest that the high propeller twist, which facilitates interplanar hydrogen bonding between bases, leads to the long-lived state observed in Ag–dC<sub>20</sub>.

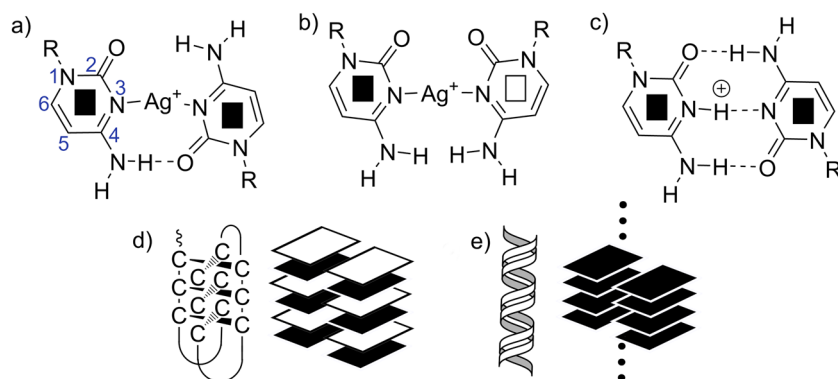


**FIG. 1.** Silver ion-mediated cytosine–cytosine base pairs in *trans* (a) and *cis* conformation (b) and the hemi-protonated C–C base pair (c). The face of each base is labeled by a black square or a white square to indicate the face seen by the viewer, according to the convention in Ref. 32 (see Ref. 33 for an alternative convention). *Trans* cytosine base pairs can form an i-motif structure in which nearest base pairs face in opposite directions (d) or a parallel-stranded duplex in which all base pairs face in the same direction (e).

## II. EXPERIMENTAL METHODS

### A. Sample preparation

dC<sub>20</sub> was purchased from the Midland Certified Reagent Company. It was purified using a gel-filtration column by the supplier and delivered as a lyophilized sample that was used as received. The amount of oligonucleotide in moles was quantified by the supplier using the absorbance of the sample in aqueous solution at 260 nm and an extinction coefficient for dC of 7400 M<sup>-1</sup> cm<sup>-1</sup>.<sup>34</sup> The dC<sub>20</sub> samples for UV-vis TA were prepared by dissolving 280 nmol of lyophilized dC<sub>20</sub> in 3 ml water. The final concentration was 1.8 mM in nucleobase (Cytosine, or Cyt). For i-dC<sub>20</sub> and ss-dC<sub>20</sub>, the pH was adjusted to pH 5.5 and pH 8.5 using HCl and NaOH, respectively.

Ag-dC<sub>20</sub> was prepared by adding 27  $\mu$ l of 100 mM AgNO<sub>3</sub> (Sigma Aldrich) to 3 ml of pH 8.5 ss-dC<sub>20</sub> solution, yielding concentrations of 0.9 mM Ag<sup>+</sup> and 1.8 mM Cyt, corresponding to a silver ion to nucleobase ratio, defined as  $\beta$ , of 0.5. The pH of the Ag-dC<sub>20</sub> samples for all measurements was 8.5 as silver nitrate addition did not change the pH. For the monomer experiments, Ag<sup>+</sup> ions were added to a cytosine (Sigma Aldrich) solution (Ag-Cyt). The final concentration was 10 mM Ag<sup>+</sup> and 20 mM Cyt ( $\beta = 0.5$ ), pH 7. The tenfold higher concentration of the nucleobase in this sample compared to the Ag-dC<sub>20</sub> sample ensured that essentially all added Ag<sup>+</sup> ions are bound (see Sec. IV A for details). Samples were not thermally annealed. All chemicals were used as received, and all solutions were prepared using ultrapurified (18 M $\Omega$ ) water from a water purifier (EMD Millipore).

### B. Steady-state spectroscopy

UV-visible absorption and CD spectra were recorded using a JASCO J-815 CD spectrometer from solutions held in a 1 mm path length fused silica cuvette. These spectra were obtained by averaging two scans recorded at a scan speed of 100 nm/min and a bandwidth of 1 nm. The dC<sub>20</sub> solutions used were 1.28 mM in cytosine nucleotides and 0.64 mM Ag<sup>+</sup>. Each CD spectrum was corrected for background using the CD spectrum recorded on neat water in the same sample cuvette. For UV-vis spectra, the measured absorbance values were converted to an effective molar absorption coefficient ( $\epsilon$ ) of the mixture by dividing by the concentration in nucleobases and the optical pathlength. All CD spectra are reported as the change in the molar extinction coefficient,  $\Delta\epsilon = \epsilon_L - \epsilon_R = \frac{\theta_{CD}}{32.98^\circ} \left( \frac{1}{cL} \right)$ , where  $\theta_{CD}$  is the raw CD signal in degrees,  $c$  is the concentration in nucleobases, and  $L$  is the optical pathlength.

### C. Silver electrode measurements

Free Ag<sup>+</sup> ion concentrations were measured using a silver ion electrode (Mettler Toledo perfection comb Ag/S2 Lemo Combination Electrode) with a minimum ion sensitivity of  $5 \times 10^{-6}$  M. The electrode was calibrated using  $10^{-5}$  M,  $10^{-4}$  M,  $10^{-3}$  M,  $10^{-2}$  M, and  $10^{-1}$  M AgNO<sub>3</sub> solutions prepared by serial dilution immediately before measuring. Solutions were stirred for 1 min–2 min after addition of each aliquot of 100 mM AgNO<sub>3</sub> solution. The voltages of the solutions were converted to concentration using the calibration curve. The bound Ag<sup>+</sup> ion concentration was calculated from the total silver ion concentration minus the unbound Ag<sup>+</sup> ion

concentration measured with the electrode ( $[Ag^+]_{bound} = [Ag^+]_{total} - [Ag^+]_{unbound}$ ).

### D. Femtosecond transient absorption spectroscopy

Broadband femtosecond TA measurements were conducted using a previously described instrument equipped with UV-visible (UV-vis) and visible-near infrared (vis-NIR) detectors.<sup>35,36</sup> Broadband TA spectra were composite spectra recorded using two different supercontinuum pulses: 320 nm–670 nm (UV-vis) generated by focusing a small fraction of the 800 nm fundamental (7.5 mJ, 80 fs, 1 kHz; Astrella, Coherent, Inc.) into a 5 mm CaF<sub>2</sub> window and 630 nm–1500 nm (vis-NIR) generated by focusing a small fraction of the 1900 nm idler from an optical parametric amplifier (TOPAS-Prime, Coherent, Inc.) into a 5 mm YAG plate. The spectra in the two regions, which were measured using identical pump fluence, were scaled to match in the overlapping region before averaging. The 265 nm pump beam, generated from a second optical parametric amplifier (TOPAS-Prime, Coherent, Inc.), was focused to a  $1/e^2$  Gaussian beam radius of  $520 \pm 50$   $\mu$ m (measured by the knife-edge scanning method) for the UV-vis experiments and  $600 \pm 60$   $\mu$ m for the vis-NIR experiments, using fused silica lenses. The pump pulse energy was adjusted by a fused silica variable neutral density filter to give a fluence of  $340 \pm 70$   $\mu$ J cm<sup>-2</sup> (assuming a Gaussian pulse) for every measurement. For all TA measurements, the angle between the electric fields of the linearly polarized pump and probe pulses was set to magic angle (54.7 $^\circ$ ) using a broadband half waveplate (AR coated for 260 nm–400 nm; Thorlabs) placed in the pump beam path. In all experiments, the sample solution was recirculated using a liquid flow cell (Harrick Scientific Products, Inc.) with a PTFE spacer (1 mm for all dC<sub>20</sub> samples; 100  $\mu$ m for both Cyt samples) placed between two CaF<sub>2</sub> windows. The Cyt solutions studied had tenfold higher nucleobase concentrations than the dC<sub>20</sub> solutions, necessitating the thin path length in the former case to achieve the same absorbance at the pump wavelength.

Although silver ion-containing samples exposed to high-intensity femtosecond laser pulses are often photolabile, only a small decrease of  $\sim 10\%$  in the absorbance of the samples with added silver nitrate was seen in UV-vis absorption spectra recorded before and after transient absorption measurements (Figs. S1 and S2). A similar decrease was measured for the silver-free i-motif sample, i-dC<sub>20</sub>, whereas no decrease was noted for the 20 mM cytosine sample. Additionally, it has been shown that silver-bound dC<sub>*n*</sub> strands have high thermal stability.<sup>28</sup>

Global fitting of the two-dimensional TA data from 500 fs to 3.4 ns was performed using the Glotaran software package.<sup>37</sup> The ss-dC<sub>20</sub>, i-dC<sub>20</sub>, Cyt, and Ag-Cyt data were fit to a biexponential function plus an offset [ $\Delta A = A_1 \exp(-t/\tau_1) + A_2 \exp(-t/\tau_2) + A_3$ ], and the Ag-dC<sub>20</sub> data were fit to a triexponential function plus an offset [ $\Delta A = A_1 \exp(-t/\tau_1) + A_2 \exp(-t/\tau_2) + A_3 \exp(-t/\tau_3) + A_4$ ], where  $A_i$  and  $\tau_i$  represent amplitudes and time constants, respectively. The reported uncertainties are twice the standard deviation ( $2\sigma$ ) estimated from the fit residuals unless this resulted in a value less than the instrument response function of the instrument of  $\sim 200$  fs. When this was the case, the uncertainty was conservatively reported as 200 fs.

## III. COMPUTATIONAL METHODS

Various structures consisting of one or more  $\text{CH}^+-\text{C}$  or  $\text{C}-\text{Ag}^+-\text{C}$  base pairs were optimized using density functional theory (DFT). In particular, the M052X functional<sup>38,39</sup> combined with the def2-svp basis set and a pseudopotential for Ag were used.<sup>40</sup> Bulk solvent effects were included using the Polarizable Continuum Model (PCM).<sup>41,42</sup> CD spectra were computed from transition energies and rotatory strengths obtained from time-dependent DFT (TDDFT). All calculated CD signals are graphed as “CD rotatory strength,” where one CD rotatory (velocity) strength unit is equal to  $10^{-40}$  erg esu cm Gauss<sup>-1</sup>. Here, we are not interested in a direct comparison of computational and experimental CD signal strengths, but by presenting all calculated CD spectra in common units, the calculated signal strengths can be meaningfully compared. This approach has yielded excellent agreement with experimental CD spectra.<sup>43–45</sup> More details are given in the [supplementary material](#)

## IV. RESULTS AND DISCUSSION

## A. Steady-state spectra and silver ion binding

The absorption spectrum of  $\text{dC}_{20}$  at pH 8.5 (ss- $\text{dC}_{20}$ ) has a long-wavelength maximum at 270 nm [Fig. 2(a), red trace]. The i- $\text{dC}_{20}$  sample at pH 5.5 peaks at 274 nm [Fig. 2(a), blue trace] and has a red tail extending to longer wavelengths compared to ss- $\text{dC}_{20}$ . The Ag- $\text{dC}_{20}$  sample at pH 8.5 [Fig. 2(a), gray trace] exhibits more

red tailing above 320 nm than the other two samples, but the long wavelength maximum is indistinguishable within experimental uncertainty from that of ss- $\text{dC}_{20}$ . The increased absorbance by Ag- $\text{dC}_{20}$  compared to the other two samples at  $\lambda < 240$  nm is due to absorption by nitrate ions from the added  $\text{AgNO}_3$ . However, this contribution is negligible at longer wavelengths where nitrate ion absorbs only weakly ( $<100 \text{ M}^{-1} \text{ cm}^{-1}$  at  $\lambda > 240 \text{ nm}$ ).<sup>46</sup> The absorption spectrum of the cytosine monomer at a concentration of 20 mM [Fig. 2(b)] is very similar with (gray) and without (red) added silver ion. No CD signal is observed before or after addition of the silver ion to the cytosine solution (Fig. S3).

The CD spectrum of  $\text{dC}_{20}$  at pH 8.5 (ss- $\text{dC}_{20}$ ) has a positive band with a maximum at 283 nm and weak negative bands at 231 nm and 213 nm [Fig. 2(c), red]. The spectrum closely resembles the previously published CD spectra of  $\text{dC}_n$  sequences in single-stranded conformation with  $n = 2$ –10 at pH 9,<sup>47</sup>  $n = 6$  at pH 7,<sup>28</sup> and  $n = 30$  at pH 8.5.<sup>17,48</sup> A similar spectrum is also seen for poly(dC) at 70 °C.<sup>49</sup> At pH 5.5, the CD spectrum of  $\text{dC}_{20}$  [Fig. 2(c), blue] shows typical i-motif features (positive peak at 287 nm and negative peak at 264 nm),<sup>17,47</sup> confirming the formation of i-motif. For i- $\text{dC}_{20}$ , the  $\Delta\epsilon$  values of 12 and  $-5 \text{ M}^{-1} \text{ cm}^{-1}$  are measured for the positive peak at 287 nm and the negative one at 263 nm, respectively.

The CD spectrum of Ag- $\text{dC}_{20}$  [Fig. 2(c), gray] is strikingly different from the CD spectra of ss- $\text{dC}_{20}$  and i- $\text{dC}_{20}$  [Fig. 2(c), red and blue, respectively]. The former signal is mostly monosignate and dominated by two strong negative bands with minima at 215 nm and 267 nm [Fig. 2(c), gray trace]. Both bands occur at roughly

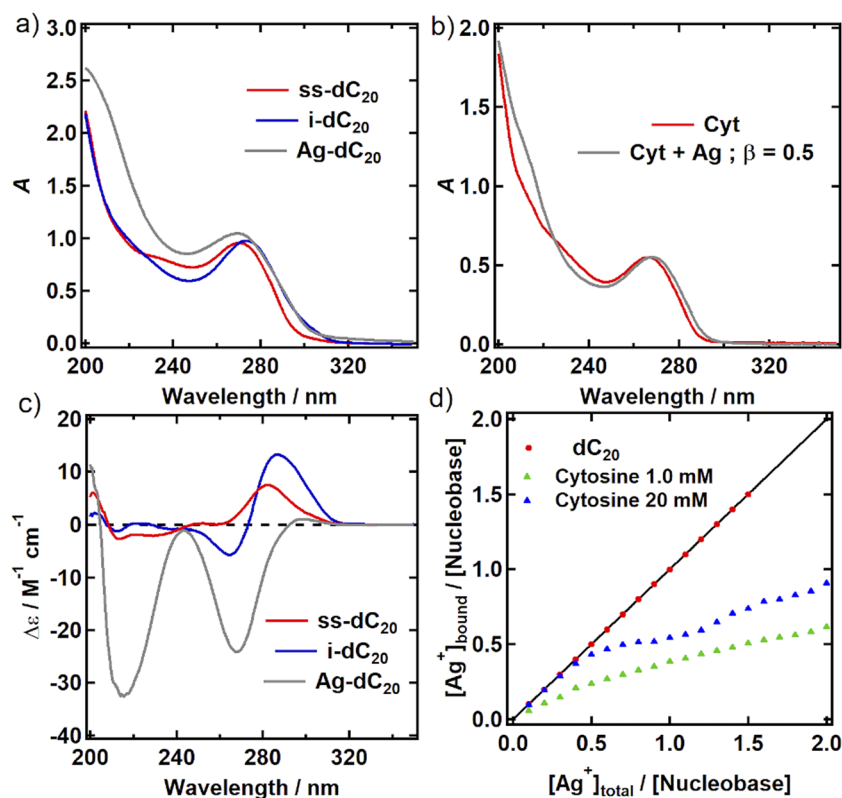


**FIG. 2.** (a) UV-vis spectra of single-stranded  $\text{dC}_{20}$  at pH 8.5 (ss- $\text{dC}_{20}$ ; red), i-motif  $\text{dC}_{20}$  at pH 5.5 (i- $\text{dC}_{20}$ ; blue), and silver-bound  $\text{dC}_{20}$  (Ag- $\text{dC}_{20}$ ,  $\beta = 0.5$ , at pH 8.5; gray). (b) UV-vis spectra of 20 mM cytosine (Cyt) and 20 mM Ag-Cyt at  $\beta = 0.5$ . (c) CD spectra of the samples shown in panel (a). (d) The concentration of  $\text{Ag}^+$  bound to Cyt ( $[\text{Ag}^+]_{\text{bound}}$ ) vs the initial  $\text{Ag}^+$  concentration ( $[\text{Ag}^+]_{\text{total}}$ ) for  $\text{dC}_{20}$  (2 mM per Cyt, red) and Cyt monomer (1.0 mM, green; 20 mM, blue) in  $\text{H}_2\text{O}$ , normalized by the Cyt concentration. The black line of unit slope illustrates 100% binding.



the same wavelengths where peaks are seen in the absorption spectrum [gray traces in Figs. 2(a) and 2(c)]. With  $\Delta\epsilon$  values of  $-32\text{ M}^{-1}\text{ cm}^{-1}$  and  $-24\text{ M}^{-1}\text{ cm}^{-1}$  measured for the negative peaks at 215 nm and 267 nm, respectively, the CD spectrum of Ag-dC<sub>20</sub> is more intense than that of i-dC<sub>20</sub> [Fig. 2(c), blue trace]. The Ag-dC<sub>20</sub> CD signals are furthermore many times more intense than those of the mononucleotide cytidine 5'-monophosphate (5'-CMP) (Fig. S4). Previously, Gwinn and co-workers reported CD spectra that are monosignate over a significant wavelength range for a variety of silver-bound DNA sequences that template AgCs, both before and after chemical reduction.<sup>50</sup>

The distinctive CD spectrum of Ag-dC<sub>20</sub> could arise from changes in conformation and/or from changes in the lowest energy electronic transitions of C upon Ag<sup>+</sup> ion binding. The former effects appear to dominate because only small changes are observed in the UV-vis spectrum of the Ag<sup>+</sup> cytosine complexes [Fig. 2(b)], suggesting that the underlying bright transitions are perturbed weakly. This agrees with gas-phase results showing that the transition energies of the C-Ag<sup>+</sup>-C complex hardly differ from those of C.<sup>51</sup>

The CD spectrum of Ag-dC<sub>20</sub> is similar to the one reported by Swasey and Gwinn<sup>29</sup> for dC<sub>20</sub> with  $\beta = 1$  (i.e., with twice our silver ion-to-nucleobase ratio). Compared to our spectrum [Fig. 2(c), gray trace], the minima of the negative peaks in the spectrum in Fig. 6(a) of Ref. 29 are shifted a few nm to longer wavelengths, and a weak, positive band is seen between the two negative features at 245 nm. These changes may be due to the different  $\beta$  values or to the  $\sim 10$ -fold higher strand concentrations in our measurements than in many of the ones in Ref. 29. Interestingly, a spectrum reported by Swasey and Gwinn for Ag<sup>+</sup> and dC<sub>20</sub> ( $\beta = 1$ ) in the presence of 100 mM NaCl matches our spectrum more closely.

Many C-rich sequences complexed with silver ions have CD spectra that are essentially identical to that of the Ag-dC<sub>20</sub> solution (see Fig. S5 and the associated text in Sec. S.2 of the [supplementary material](#)). Some of these systems have been described as Ag-i-motif structures, while others were reported to be parallel-stranded duplex structures. The virtually identical CD spectra observed for all of these C-rich, but sequence-diverse systems strongly suggest that they share a common conformational motif. As discussed below, we believe that this motif involves stacks of consecutive C-Ag<sup>+</sup>-C base pairs with a left-handed propeller twist in a right-handed double helix.

The ratio of bound silver ions to nucleobase is graphed vs  $\beta$  in Fig. 2(d). For the dC<sub>20</sub> solution [Fig. 2(d), red circles], the concentration of free silver ions is below the detection limit (5  $\mu\text{M}$ ) for  $\beta$  values between 0 and 1.5, the highest value studied, indicating that  $>99.5\%$  of all Ag<sup>+</sup> ions are bound to dC<sub>20</sub> for the  $\beta = 0.5$  solutions used in the TA experiments described below. For the cytosine monomer solutions, most of the data points fall below the line of unit slope in Fig. 2(d), indicating that not all Ag<sup>+</sup> ions form nucleobase complexes. Stronger binding is observed over the entire range of  $\beta$  values for the 20 mM Cyt solution than for the 1 mM Cyt solution [Fig. 2(d), blue vs green triangles] with virtually all Ag<sup>+</sup> ions bound for  $\beta = 0.5$ . The 1:2 stoichiometry of bound Ag<sup>+</sup> ions to C for the systems of interest here is consistent with C-Ag<sup>+</sup>-C base pairing but could obviously accommodate other structural motifs. Based on strong evidence that Ag<sup>+</sup> binds to the N3 atoms of two cytosines,<sup>52</sup> our calculations assume this as a starting point and focus on interactions among C-Ag<sup>+</sup>-C base pairs.

## B. Computed CD spectra

### 1. H-i-motif and Ag-i-motif

Lopez-Acevedo and co-workers calculated the CD spectrum of two stacked C-Ag<sup>+</sup>-C base pairs,<sup>53</sup> but there has been no computational modeling of the CD spectrum of the H-i-motif to the best of our knowledge. An initial calculation of the CD spectrum of an H-i-motif structure (Fig. S6) for comparison with the well-known, experimental CD spectrum was performed to calibrate our theoretical approach before applying it to the silver ion-mediated base pairs.

In the computed CD spectrum of the H-i-motif (Fig. S7, blue curve), three peaks are seen at 280 nm (positive), 256 nm (negative), and 222 nm (positive). Overall, the spectrum compares well with the experimental spectrum of i-dC<sub>20</sub> [Fig. 2(c), blue trace]. The positive peak near 220 nm in the computed spectrum is very weak in our experimental spectrum but is more prominent in the published CD spectra of i-motif structures formed by other dC<sub>n</sub> sequences.<sup>17,47,54</sup> The calculated spectrum also reproduces well the weak shoulder on the high energy side of the negative band near 260 nm with its characteristic inflection point at  $\sim 240$  nm. This good agreement suggests that the level of theory used in these preliminary calculations is sufficient for robustly identifying major spectral features.

The structure of a hypothetical Ag-i-motif is shown in Figs. S6b and S6d. The calculated CD spectrum of this structure (Fig. S7, red curve) has a qualitatively similar pattern of alternating positive and negative peaks as for the H-i-motif but clearly differs from the experimental CD spectrum of Ag-dC<sub>20</sub> [Fig. 2(c), gray trace]. The calculation thus fully supports conclusions from recent experiments<sup>55</sup> and calculations<sup>56</sup> that dC<sub>n</sub> sequences with added Ag<sup>+</sup> ions do not form i-motif-like structures. To study more efficiently the possible structures responsible for the CD spectrum of Ag-dC<sub>20</sub>, we focused our calculations on a less demanding system, i.e., a tetramer of two C-Ag<sup>+</sup>-C base pairs (C-Ag<sup>+</sup>-C)<sub>2</sub>, as discussed next.

### 2. C-Ag<sup>+</sup>-C base pair steps: Structures

The geometry optimized structures of two *trans* C-Ag<sup>+</sup>-C base pairs stacked as in a parallel-stranded duplex (structure I) and as in the hypothetical Ag-i-motif structure (structure II) were studied computationally (Fig. 3 and Fig. S8). In the latter structure, the *trans* base pairs face in alternate directions as in the H-i-motif [Fig. 1(d)]. Short Ag-Ag distances are found in both structure I (2.97 Å) and structure II (3.03 Å), indicating significant argentophilic interactions as seen in a number of crystal structures of silver ion-mediated base pairs between cytosines and cytosine derivatives.<sup>10,21–23</sup>

Structure I is very similar to the C-Ag<sup>+</sup>-C base pairs seen in the crystal structure reported by Huard *et al.*<sup>23</sup> of a fluorescent silver cluster templated by parallel joining of the DNA sequence d(A<sub>2</sub>C<sub>4</sub>) (PDB identifier 6NIZ). Fluorescent silver clusters formed by chemical reduction of complexes formed between DNA strands and silver nitrate, of course, contain significant quantities of Ag<sup>0</sup> atoms, but Huard *et al.*<sup>23</sup> noted that superimposable crystal structures are observed before and after reduction of Ag<sup>+</sup> to Ag<sup>0</sup>.<sup>23</sup> Like the consecutive C-Ag<sup>+</sup>-C base pairs detected in the stem region of the structure determined in Ref. 23, the two base pairs in structure I exhibit

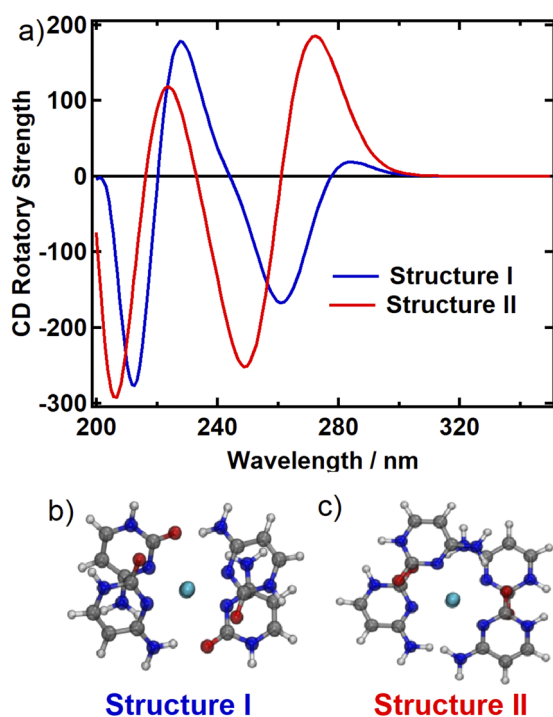


**FIG. 3.** (a) Calculated CD spectra of two *trans* C–Ag<sup>+</sup>–C base pairs oriented as in a parallel duplex (structure I, blue curve) and in an i-motif-like manner (structure II, red curve). (b) and (c) Optimized geometries of structures I and II. Atom coloring scheme: C (gray), H (white), O (red), N (blue), and Ag (cyan).

high propeller twist (see Ref. 57 for a definition) of slightly more than  $-40^\circ$  (Fig. S8a).

The propeller twist, which is left-handed like the propeller twist observed in most double-stranded DNAs,<sup>58</sup> allows structure I to form distinctive inter-base pair (“diagonal”) hydrogen bonds between the carbonyl group of each cytosine in a C–Ag<sup>+</sup>–C base pair and the amino group of a cytosine on the opposite strand in the adjacent C–Ag<sup>+</sup>–C base pair (Fig. 4). Similar diagonal hydrogen bonds were first reported in calculations by Espinosa Leal *et al.*<sup>53</sup> and then observed in crystal structures containing C–Ag<sup>+</sup>–C base pairs.<sup>10,21–23</sup> As discussed by Müller,<sup>8</sup> high propeller twist allows both metal–nucleobase coordinate bonds and the formation of hydrogen bonds between adjacent base pairs. This geometry maintains well-stacked bases on each strand, as illustrated in Fig. 4, and this is likely to be a key to the excited-state dynamics discussed below. In structure II, each C–Ag<sup>+</sup>–C base pair has minimal propeller twist and is nearly planar as measured by dihedral angles C2–N3–N3′–C2′ of  $176^\circ$  for both base pairs. The O2–C2–C2′–O2′ dihedral angle between the two carbonyl groups that are nearest to each other is  $180^\circ$ .

### 3. C–Ag<sup>+</sup>–C base pair steps: CD spectra

The CD spectra of structures I and II are compared in Fig. 3(a). The predicted CD spectrum of structure I [Fig. 3(a), blue curve] has two negative peaks at 215 nm and 260 nm that agree well with

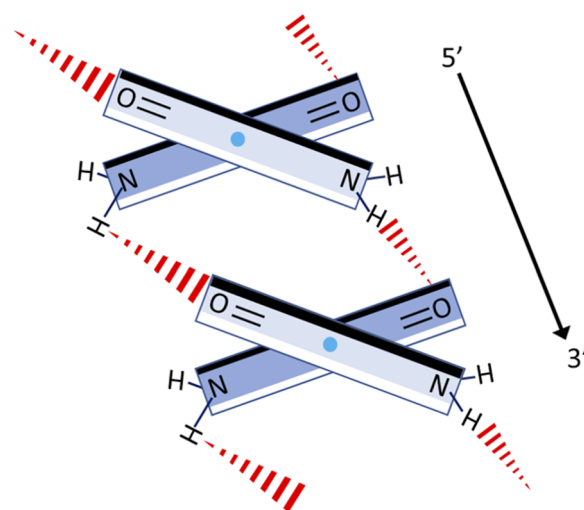


**FIG. 4.** A model of the dC<sub>20</sub> metallo DNA structure, which is stabilized by *trans* base pairs with high propeller twist that enable the inter-base pair hydrogen bonds shown by the dashed, red wedges (side-on view, looking along the N3–N3′ axis; silver ions are shown by cyan circles). Carbonyl and amino groups of the Watson–Crick face of each cytosine are shown. These groups are located on the edge of each base closest to the silver ion that joins them.

the twin negative bands seen for Ag–dC<sub>20</sub> at 215 nm and 267 nm [Fig. 2(c), gray trace]. While the calculated CD spectrum of structure II [Fig. 3(a), red curve] also shows a pair of negative peaks, these are shifted to 207 nm and 250 nm and agree less well with the Ag–dC<sub>20</sub> spectrum. Both the calculated CD spectra in Fig. 3 have a positive peak between the negative signals. Although a positive feature is not seen in our CD spectrum of Ag–dC<sub>20</sub> in this region, a weak positive band has been reported near 245 nm in the CD spectra of several cytosine-rich DNA strands complexed with Ag<sup>+</sup> ions.<sup>15,29</sup> Evidence in Ref. 29 suggests that the amplitude of this peak decreases under conditions that favor DNA aggregation, but this was not a focus of our study.

Overall, the CD spectrum of structure I agrees well with the “universal” CD spectrum seen in many C-rich sequences with bound silver ions as discussed in Sec. IV A. In addition to the twin negative bands found between 200 nm and 280 nm, we note that the calculated CD spectrum of structure I agrees much better with the CD spectrum of Ag–dC<sub>20</sub> above 240 nm. Only structure I has a weak positive peak at 290 nm that matches the experiment, while the structure II CD spectrum predicts a strong positive band at 275 nm and a zero crossing near 260 nm, neither of which is seen in the experimental CD spectrum of Ag–dC<sub>20</sub>. The good agreement of the structure I CD spectrum with that of Ag–dC<sub>20</sub> strongly suggests that propeller-twisted, stacked C–Ag<sup>+</sup>–C base pairs like the ones illustrated in Fig. 4 are present in these parallel-stranded duplexes. We determined further that the CD spectrum calculated for the mirror image of structure I is opposite in sign to the blue curve in Fig. 3(a), confirming that the Ag–dC<sub>20</sub> system forms a right-handed helix of stacked C–Ag<sup>+</sup>–C base pairs with left-handed propeller twist.

To investigate the origin of the CD signals further, calculations were performed on single base pairs after geometry optimization and with the geometry found in structure I. Only very weak CD signals are predicted for single  $\text{CH}^+-\text{C}$  and  $\text{C}-\text{Ag}^+-\text{C}$  base pairs (Fig. S10) as expected from their nearly planar geometries (Fig. S9) that result in coplanar transition dipole moments for the important in-plane transitions. The calculated CD spectrum for a single, propeller-twisted  $\text{C}-\text{Ag}^+-\text{C}$  base pair extracted from structure I is more intense (Fig. S11) but lacks the twin negative bands seen in the CD spectrum of  $\text{Ag}-\text{dC}_{20}$  [Fig. 2(c), gray curve]. This indicates that both propeller twisting and C-C intrastrand stacking are important, possibly because the excitonic state is delocalized over two  $\text{C}-\text{Ag}^+-\text{C}$  base pairs.

## C. Broadband transient absorption spectra

### 1. $\text{dC}_{20}$ systems

The TA spectra of ss- $\text{dC}_{20}$ , i- $\text{dC}_{20}$ , and  $\text{Ag}-\text{dC}_{20}$  recorded with 265 nm excitation are compared in Fig. 5. The broadband TA spectra of  $\text{dC}_n$  sequences with  $n > 2$ , whether in single strand or i-motif form, have not been reported previously to the best of our knowledge. The TA spectrum for ss- $\text{dC}_{20}$  at 1 ps shows strong absorption in the UV below 350 nm, a dip at 360 nm, and broad absorption throughout the visible and NIR [Fig. 5(a)]. The TA signals from ss- $\text{dC}_{20}$  and i- $\text{dC}_{20}$  have recovered to zero or a weak offset by 3 ns after the excitation pulse [Figs. 5(a) and 5(b)]. In contrast, the  $\text{Ag}-\text{dC}_{20}$  transient spectrum at 3 ns rises monotonically from the NIR toward

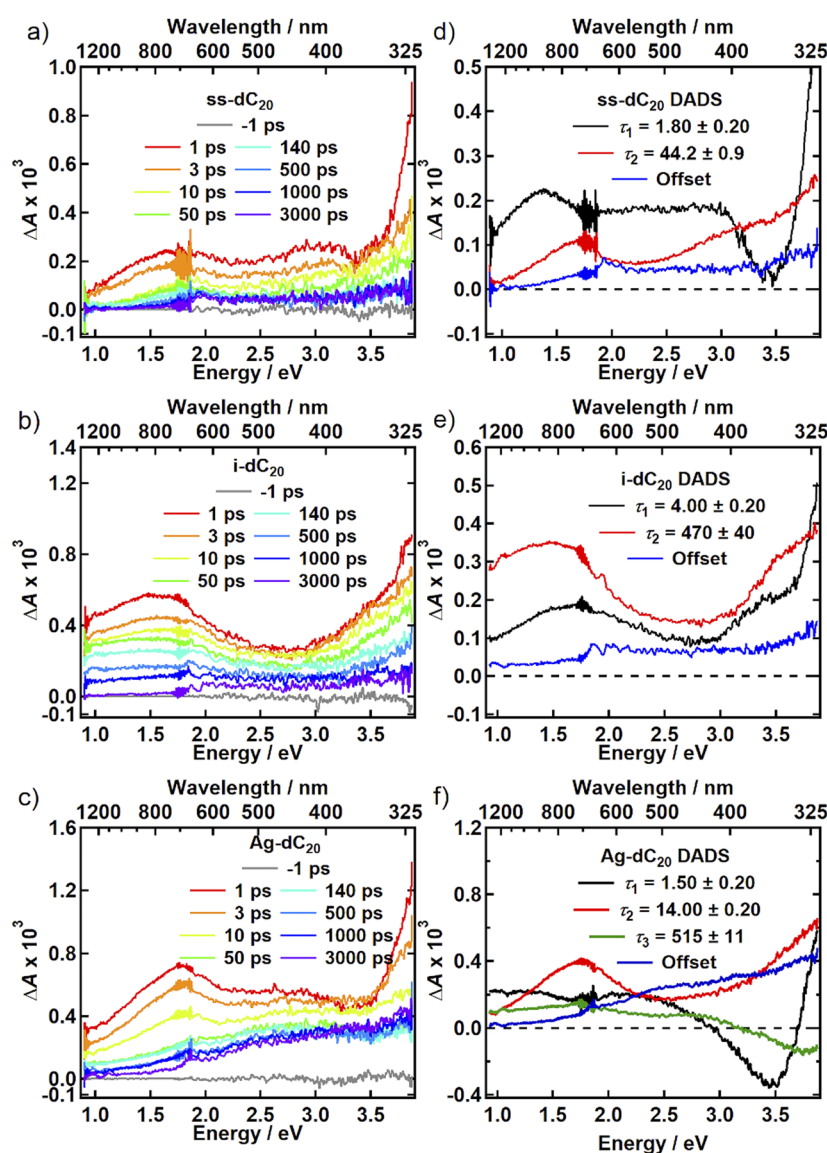


**FIG. 5.** Transient absorption spectra of (a) ss- $\text{dC}_{20}$ , (b) i- $\text{dC}_{20}$ , and (c)  $\text{Ag}-\text{dC}_{20}$  in  $\text{H}_2\text{O}$  at selected delay times after 265 nm excitation. The decay associated difference spectra (DADS) obtained from global fitting of the data for (d) ss- $\text{dC}_{20}$ , (e) i- $\text{dC}_{20}$ , and (f)  $\text{Ag}-\text{dC}_{20}$ .



the UV. This spectral component, which is absent in ss-dC<sub>20</sub> and i-dC<sub>20</sub> [Figs. 5(a) and 5(b)], is largely unchanged from 1 ns to 3.5 ns, the detection limit of our instrument [Fig. 5(c)].

The time- and probe wavelength-dependent TA signals were fit between 500 fs and 3.4 ns using sums of exponential functions with time constants that were globally linked at all probe wavelengths (see the [supplementary material](#) for additional details). The time constants obtained from the fits to the dC<sub>20</sub> samples and to the Ag-Cyt signals discussed later are summarized in Table I. For ss-dC<sub>20</sub>, time constants of  $\tau_1 = 1.80$  ps and  $\tau_2 = 44.2$  ps and an offset provided the best fit [Fig. 5(d)]. The transient spectrum of ss-dC<sub>20</sub> exhibits a dip at 3.5 eV (350 nm) at 1 ps [Fig. 5(a)], which quickly disappears as seen from the fact that the dip contributes only to the decay-associated difference spectrum (DADS) of the 1.8 ps component [Fig. 5(d), black]. Both the position of the dip and its decay time are in excellent agreement with features observed for dCyd and dCMP,<sup>59</sup> and the dip is assigned to stimulated emission (SE) from short-lived excited states, many of which are proposed to localize on single bases.

The ss-dC<sub>20</sub> transient spectra exhibit a broad peak at 400 nm, which can be seen at 10 ps [Fig. 5(a), light green]. This feature is also visible in the DADS of the 44 ps component, which has a broad peak near 400 nm that merges with a stronger band at shorter wavelengths [Fig. 5(d), red]. We propose that a  $^1n\pi^*$  state is responsible based on the similar transient spectral features seen by Ma *et al.*<sup>59</sup> in their broadband femtosecond TA measurements on Cyt and CMP. Because the  $^1n\pi^*$  state population is thought to decay primarily to the ground state, the transient difference spectrum associated with this species (i.e., the SADS) is equal to the DADS of the 44 ps component. The steady decrease from 3.5 eV to 2.0 eV is in reasonable agreement with the excited state absorption spectrum calculated at the minimum of the  $^1n\pi^*$  state of dCyd.<sup>60</sup> Finally, the decay time of this state agrees with the assignment by Keane *et al.*,<sup>48</sup> who observed 50 ps–80 ps time constants for single-stranded dC<sub>2</sub>, dC<sub>30</sub>, and poly(rC) in time-resolved IR (TRIR) experiments with UV excitation.

Similar to ss-dC<sub>20</sub>, the i-dC<sub>20</sub> signals can also be modeled by a biexponential function plus an offset, but the  $\tau_2$  component is ten times longer (470 ps) than in the single strand [Fig. 5(e)]. The DADS of this component is also very different: A strong NIR band with maximum at 1.5 eV (830 nm) is seen, which is red shifted and broadened compared to the NIR band in the 44 ps component of ss-dC<sub>20</sub> [compare red traces in Figs. 5(d) and 5(e)]. Keane *et al.*<sup>18</sup> used TRIR to study the excited-state dynamics of several proton i-motif-forming sequences, including dC<sub>30</sub> and the human telomeric sequence. They observed a state with a lifetime of 200 ps–400 ps.<sup>18</sup>

For comparison, fluorescence upconversion measurements of i-dC<sub>20</sub> reveal multiexponential emission decays with an average lifetime of 257 ps.<sup>61</sup> These decay times, which are in reasonable agreement with the  $470 \pm 40$  ps decay component observed in our TA experiments on i-dC<sub>20</sub>, have been assigned to charge recombination (CR) of the CT state formed by photoinduced electron transfer from cytosine to its protonated counterpart.<sup>16,17</sup>

For Ag-dC<sub>20</sub>, the 1.5 ps and 515 ps DADS [Fig. 5(f)] possess negative amplitudes in the UV region, which indicates rising TA signals in this region (discussed below). The  $\tau_2 = 14$  ps DADS for Ag-dC<sub>20</sub> is very similar in appearance to the  $\tau_2 = 44$  ps DADS seen for ss-dC<sub>20</sub>, which we also assign to the SADS of a  $^1n\pi^*$  excited state. As both spectra feature a broad band near 720 nm (1.7 eV), which is similar in appearance to the absorption spectrum of the hydrated electron, we carefully considered the possibility of photoionization. However, one-photon ionization of these solutes by the 265 nm pump pulse is not expected given the high vertical ionization potential of cytosine ( $\sim 8.0$  eV).<sup>62</sup> Although a water-only scan measured back-to-back with identical experimental parameters yields a weak hydrated electron signal due to two-photon ionization of water (Fig. S12a), this signal contribution would be attenuated significantly by the high one-photon absorbance of our solution at the pump wavelength ( $A_{265} = 1.5$ ) and thus cannot account for the intensity of the observed visible–NIR band.

## 2. Cyt and Ag-Cyt

To better understand the long-lived state observed in Ag-dC<sub>20</sub>, experiments were performed on the silver-cytosine complex (Ag-Cyt) formed by adding silver nitrate to an aqueous solution of 20 mM cytosine. The high monomer concentration increased the binding of Ag<sup>+</sup> ions to Cyt [compare blue and green triangles in Fig. 2(d)], thereby reducing the background signal from uncomplexed Cyt. The TA spectra of the 20 mM Cyt solution without silver ions [Fig. 6(a)] show strong absorption at the shortest UV wavelengths probed, which decreases with increasing wavelength, revealing a distinctive peak at 3.0 eV (410 nm). The TA spectra of the Ag-Cyt solution [Fig. 6(b)] are similar to those of Cyt [Fig. 6(a)] at probe energies greater than 2.5 eV ( $<500$  nm), but the Ag-Cyt spectra feature a broad positive band with a maximum near 2 eV (600 nm) that extends past the low-energy edge of our detection window at 0.9 eV (1400 nm). The TA spectra of 20 mM Cyt feature minimal absorption at wavelengths greater than 2.0 eV (600 nm), although a very weak and broad absorption band is discernible at 1.3 eV (950 nm) in the DADS spectrum of the shortest decay component ( $\tau = 0.650$  ps) [Fig. 6(c)]. Overall, the TA spectra agree well with ones recorded by Ma *et al.*<sup>59</sup> with broadband probing

TABLE I. Time constants (ps) obtained from global fitting to the dC<sub>20</sub> and Cyt data shown in Figs. 5 and 6, respectively.

	ss-dC <sub>20</sub>	i-dC <sub>20</sub>	Ag-dC <sub>20</sub>	Cyt	Ag-Cyt
$\tau_1$	$1.80 \pm 0.20$	$4.00 \pm 0.20$	$1.47 \pm 0.20$	$0.65 \pm 0.20$	$0.60 \pm 0.20$
$\tau_2$	$44.2 \pm 0.9$	$470 \pm 40$	$13.96 \pm 0.20$	$6.14 \pm 0.20$	$13.06 \pm 0.20$
$\tau_3$	Offset	Offset	$515 \pm 11$	Offset	Offset
$\tau_4$	...	...	Offset	...	...

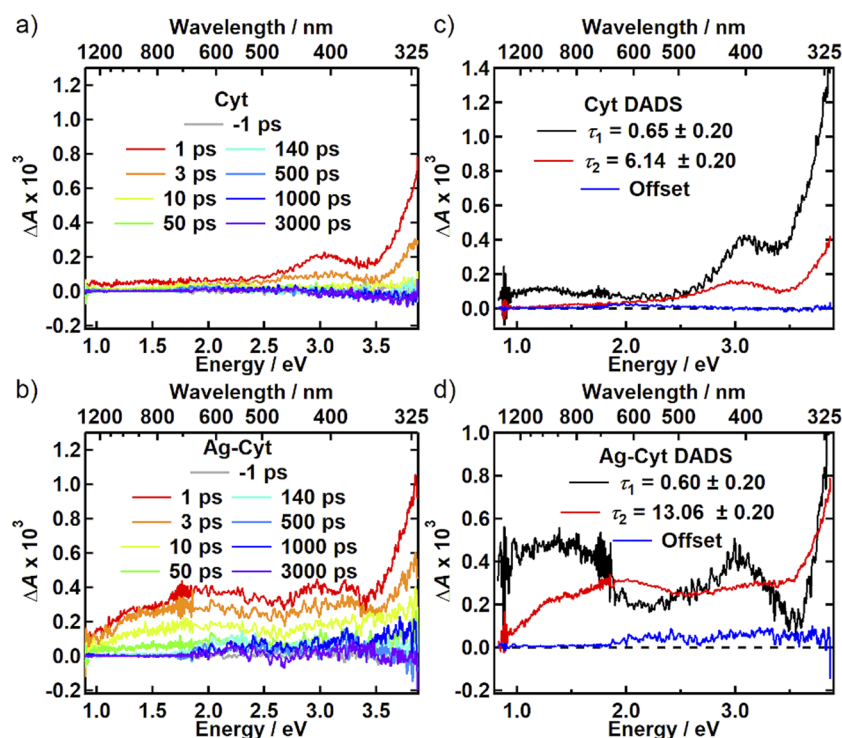


FIG. 6. TA spectra of (a) 20 mM Cyt and (b) Ag-Cyt (20 mM Cyt,  $\beta = 0.5$ ) in  $\text{H}_2\text{O}$  at the indicated delay times after 265 nm excitation and DADS from global fitting to the Cyt (c) and Ag-Cyt (d).

between 280 nm and 600 nm using a five- to tenfold lower Cyt concentration.

We again rule out a contribution from hydrated electrons generated by two-photon ionization of water as solvent-only control experiments made with the same 100  $\mu\text{m}$  path length cell used for the Cyt and Ag-Cyt measurements produce negligible signals (Fig. S12b). The decay of the vis-NIR band in Ag-Cyt is furthermore much too rapid compared to the geminate recombination kinetics of hydrated electrons, providing strong evidence that the vis-NIR signal originates from the solute. Global fitting of the Ag-Cyt TA data reveals two decay components with time constants of 0.60 ps and 13 ps along with a very weak offset [Fig. 6(d)]. The offset seen in Ag-Cyt is very weak compared to the prominent offset seen in Ag-dC<sub>20</sub> [Fig. 5(f)]. This striking difference is easily seen in the temporal evolution of the TA signals, as discussed in Sec. IV D.

The TA spectra and decay kinetics of Ag-Cyt [Figs. 6(b) and 6(d)] are similar to those of ss-dC<sub>20</sub> [Figs. 5(a) and 5(d)], with the exception that the absorption in the 500 nm–1400 nm region is stronger in Ag-Cyt. We note that the changes seen with Ag<sup>+</sup> ion addition to cytosine (broad visible absorption at early times and the presence of a  $\sim 30$  ps decay) are reminiscent of those seen by Ma *et al.*<sup>59</sup> upon addition of a (phospho)ribose group to the N1 position of cytosine, suggesting that silver binding to cytosine has similar effects. Interestingly, photoexcitation of the gas-phase complex of Cyt with a single Ag<sup>+</sup> ion leads to the detection of the Cyt radical cation.<sup>63</sup> Future experiments are needed to investigate the possibility of photoinduced ET reactions in the putative Cyt-Ag<sup>+</sup>-Cyt complex in aqueous solution.

We carefully considered the possibility that AgNO<sub>3</sub> addition to the concentrated Cyt solution produces self-assembled nanostructures. Fibers 6 nm in diameter, but many  $\mu\text{m}$  in length, have been previously observed for Ag<sup>+</sup>-cytidine complexes in methanol,<sup>10</sup> and Ag<sup>+</sup> ion coordination to various cytosine monomers in aqueous solution results in crystals containing supramolecular helices.<sup>10,24,64</sup> Adding AgNO<sub>3</sub> to aqueous solutions of adenine (Ade) and its fluorescent counterpart 2-aminopurine (2AP) yields coordination polymers that assemble into nanofibers tens of nanometers in diameter and micrometers in length as revealed by atomic force microscopy (AFM).<sup>11,65</sup> For Ade and 2AP, self-assembly driven by Ag<sup>+</sup> ion coordination is accompanied by dramatic changes in UV-visible absorption (red shifts of 10 nm–30 nm, and prominent red tailing), signaling substantial electronic coupling among spatially proximal chromophores.<sup>11</sup> However, no such changes are seen in the absorption spectrum of the 20 mM Ag-Cyt solution, which red shifts by only 1 nm compared to Cyt [Fig. 1(b)]. We were furthermore unable to detect nanoscale structures of any kind by AFM imaging of films drop cast from the Ag-Cyt solution. Importantly, crystals grown from Cyt and silver nitrate have sheet-like, non-helical structures that lack short Ag-Ag distances.<sup>66</sup>

#### D. Transient absorption kinetics

Kinetic traces for the dC<sub>20</sub> samples and for the Ag-Cyt solution at  $\lambda_{\text{probe}} = 350$  nm (UV) and  $\lambda_{\text{probe}} = 1000$  nm (NIR) are shown in Fig. 7. Generally, the signals in the NIR decay faster than the ones at UV probe wavelengths. By 3 ns, the longest delay time accessible

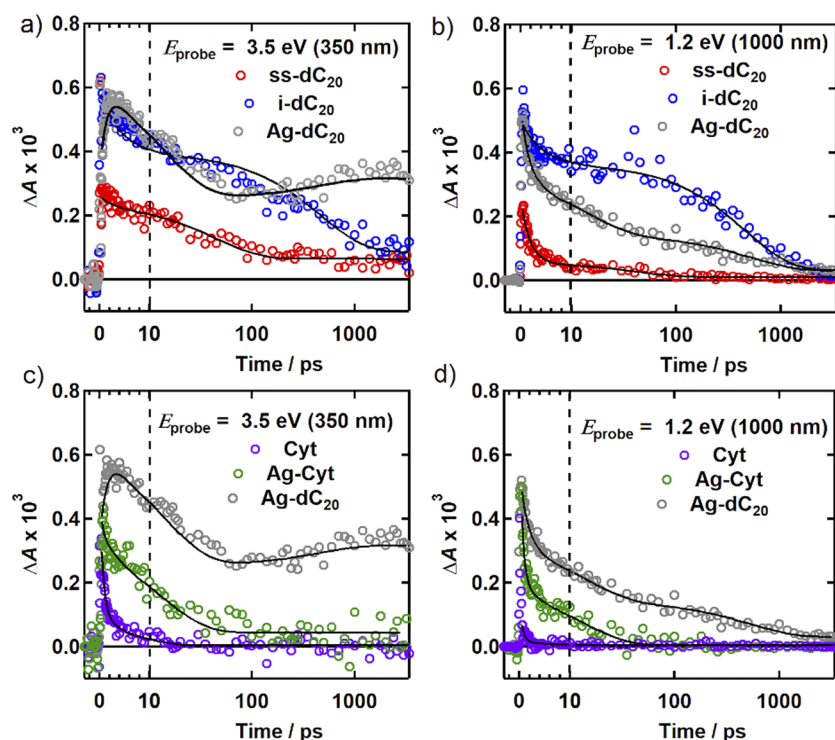


**FIG. 7.** Kinetic traces at (a)  $\lambda_{\text{probe}} = 350$  nm (3.5 eV) and (b)  $\lambda_{\text{probe}} = 1000$  nm (1.2 eV) for Ag-dC<sub>20</sub> (gray), ss-dC<sub>20</sub> (red), and i-dC<sub>20</sub> (blue) in H<sub>2</sub>O following 265 nm (4.7 eV) excitation. The gray trace for Ag-dC<sub>20</sub> is an average of 10 curves from 352 nm to 356 nm. Kinetic traces at (c)  $\lambda_{\text{probe}} = 350$  nm (3.5 eV) and (d)  $\lambda_{\text{probe}} = 1000$  nm (1.2 eV) for Cyt (purple) and the Ag-Cyt solution (green) in H<sub>2</sub>O following 265 nm (4.7 eV) excitation. The Ag-dC<sub>20</sub> traces (gray) are shown again for comparison. The markers are experimental data, and the solid curves are fits obtained from global fitting. The vertical dashed line denotes the linear-logarithmic axis break at 10 ps.

in our study, most signals have decayed to the baseline or to a weak offset that is many times weaker than the maximum signal amplitude near time zero. The notable exception is the signal from Ag-dC<sub>20</sub> probed at 350 nm [Fig. 7(a), gray circles]. This signal initially grows during the first few ps after photoexcitation, decays until  $\sim 100$  ps, but then increases to 1 ns and remains relatively constant thereafter. The multi-stage growth kinetics are manifest by the negative amplitudes seen in the 1.5 ps and 515 ps DADS of Ag-dC<sub>20</sub> at probe energies  $>3.0$  eV [Fig. 5(f)]. The near constancy of the 350 nm signal from 1 ns to 3 ns, the limit of our time window, suggests that the species responsible for the long-time spectrum is very long-lived and persists for  $>10$  ns. The ratio of the signal at 3 ns to the signal at time zero is substantial, suggesting that the yield of this channel is large.

Strikingly, the Ag-Cyt TA signal at 350 nm [Fig. 7(c)] lacks the long-lived signal seen in Ag-dC<sub>20</sub>. We propose that stacked and propeller twisted C-Ag<sup>+</sup>-C base pairs, shown above to yield the distinctive CD spectrum of Ag-dC<sub>20</sub>, give rise to the long-lived excited state in Ag-dC<sub>20</sub>. This state is not seen in Ag-Cyt, consistent with dimeric or sheet-like structures that lack stacking by C-Ag<sup>+</sup>-C base pairs.

### E. Long-lived excited states in Ag-dC<sub>20</sub>

Two possible assignments for the long-lived state in Ag-dC<sub>20</sub> are a charge separated state or a triplet state. Absorption by the cytosine radical cation is characterized by a broad band spanning 350 nm–700 nm with a maximum at 415 nm.<sup>15</sup> The cytosine radical anion absorption spectrum decreases almost monotonically from

350 nm to 700 nm with a small dip at 415 nm.<sup>67</sup> A weighted sum of these two spectra, corresponding to absorption by the charge separated species C<sup>•+</sup> and C<sup>•-</sup>, yields a nearly featureless spectrum that falls from short to long wavelengths, not unlike the spectrum of the offset in Fig. 5(f).

On the other hand, a triplet state localized on one C residue also seems likely. The triplet absorption spectrum of cytidine 5'-monophosphate from Ref. 68 decreases from 320 nm to 700 nm with a weak peak discernable near 415 nm. This spectrum is thus also very similar to the long-time TA spectrum of Ag-dC<sub>20</sub> [Fig. 5(c)]. In fact, the formation of a triplet state may be a consequence of the propensity for photoinduced charge transfer in DNA strands and the special geometry of this silver ion-mediated duplex. We note that strongly propeller-twisted base pairs are reminiscent of donor-acceptor dyads with orthogonal orbitals that enhance inter-system crossing through charge transfer-mediated mechanisms.<sup>69</sup> Further work is needed to explore this possibility, but regardless of the precise identity of the long-lived excited state, the present study establishes that silver ion-mediated base pairing yields metallo-DNA structures that have photophysical properties not found in metal-free DNA strands.

### V. CONCLUSION

Silver(I) ions bind strongly to both the cytosine monomer and dC<sub>20</sub>, giving rise to silver ion-mediated base pairs, which form quite different higher-order structures, leading to dramatic differences in excited state dynamics. Excited state deactivation in both of these

metallo-DNA systems is furthermore distinct from dynamics in ss-dC<sub>20</sub> or i-dC<sub>20</sub>. Our computational results confirm that Ag-dC<sub>20</sub> forms a parallel-stranded duplex, and we are able to show through an analysis of experimental and calculated CD spectra that a right-handed double helix is formed in which each base pair has a high propeller twist angle. It would be very interesting to study the flexibility of Ag-dC<sub>20</sub> and similar metallo-DNAs, given that high propeller twist in regular DNA sequences has been linked to reduced flexibility.<sup>58</sup> An exciting possibility is that the rigid, well-stacked structures made possible by propeller twisted base pairs promote exciton delocalization and/or charge separation.

The combined spectroscopy and theory from this study show that stacked, propeller-twisted C-Ag<sup>+</sup>-C base pairs present in Ag-dC<sub>20</sub> give rise to a long-lived, high yield state. Future studies are needed to precisely characterize this state, which we have suggested may be a triplet or long-lived charge separated state. The ability to manipulate DNA secondary and tertiary structures by metal ion binding shows considerable promise for tailoring, manipulating, and controlling the photophysical properties of DNA-templated silver clusters and other metallo-DNAs.

## SUPPLEMENTARY MATERIAL

See the [supplementary material](#) for information on sample photodegradation, additional CD spectra, full computational details, and solvent-only transient absorption signals.

## ACKNOWLEDGMENTS

The work at The Ohio State University was supported by a grant from the U.S. National Science Foundation (Grant No. CHE-1800471). L.M.-F. thanks the MINECO project (No. CTQ2016-76061-P) for financial support and the Centro de Computación Científica, CCC-UAM, for generous allocation of computational time. The authors declare no competing financial interest.

## DATA AVAILABILITY

The data that support the findings of this study are available from the corresponding author upon reasonable request.

## REFERENCES

- <sup>1</sup>J. Chen, Y. Zhang, and B. Kohler, in *Photoinduced Phenomena in Nucleic Acids II: DNA Fragments and Phenomenological Aspects*, edited by M. Barbatti, A. C. Borin, and S. Ullrich (Springer-Verlag Berlin, Berlin, 2015), pp. 39–87.
- <sup>2</sup>Y. Zhang, K. de La Harpe, A. A. Beckstead, R. Improta, and B. Kohler, “UV-induced proton transfer between DNA strands,” *J. Am. Chem. Soc.* **137**, 7059–7062 (2015).
- <sup>3</sup>D. B. Bucher, B. M. Pilles, T. Carell, and W. Zinth, “Charge separation and charge delocalization identified in long-living states of photoexcited DNA,” *Proc. Natl. Acad. Sci. U. S. A.* **111**, 4369–4374 (2014).
- <sup>4</sup>Y. Zhang, J. Dood, A. A. Beckstead, X.-B. Li, K. V. Nguyen, C. J. Burrows, R. Improta, and B. Kohler, “Efficient UV-induced charge separation and recombination in an 8-oxoguanine-containing dinucleotide,” *Proc. Natl. Acad. Sci. U. S. A.* **111**, 11612–11617 (2014).
- <sup>5</sup>Y. Zhang, J. Dood, A. A. Beckstead, X.-B. Li, K. V. Nguyen, C. J. Burrows, R. Improta, and B. Kohler, “Photoinduced electron transfer in DNA: Charge shift dynamics between 8-oxo-guanine anion and adenine,” *J. Phys. Chem. B* **119**, 7491–7502 (2015).
- <sup>6</sup>Y. Zhang, K. de La Harpe, A. A. Beckstead, L. Martínez-Fernández, R. Improta, and B. Kohler, “Excited-state dynamics of DNA duplexes with different H-bonding motifs,” *J. Phys. Chem. Lett.* **7**, 950–954 (2016).
- <sup>7</sup>J. Chen and B. Kohler, “Base stacking in adenosine dimers revealed by femtosecond transient absorption spectroscopy,” *J. Am. Chem. Soc.* **136**, 6362–6372 (2014).
- <sup>8</sup>J. Müller, “Nucleic acid duplexes with metal-mediated base pairs and their structures,” *Coord. Chem. Rev.* **393**, 37–47 (2019).
- <sup>9</sup>S. Naskar, R. Guha, and J. Müller, “Metal-modified nucleic acids: Metal-mediated base pairs, triples, and tetrads,” *Angew. Chem., Int. Ed.* **59**, 1397–1406 (2020).
- <sup>10</sup>L. Mistry, O. El-Zubir, G. Dura, W. Clegg, P. G. Waddell, T. Pope, W. A. Hofer, N. G. Wright, B. R. Horrocks, and A. Houlton, “Addressing the properties of ‘Metallo-DNA’ with a Ag(I)-mediated supramolecular duplex,” *Chem. Sci.* **10**, 3186–3195 (2019).
- <sup>11</sup>J. A. Snyder, A. P. Charnay, F. R. Kohl, Y. Zhang, and B. Kohler, “DNA-like photophysics in self-assembled silver(I)-nucleobase nanofibers,” *J. Phys. Chem. B* **123**, 5985–5994 (2019).
- <sup>12</sup>K. Gehring, J.-L. Leroy, and M. Guéron, “A tetrameric DNA structure with protonated cytosine-cytosine base pairs,” *Nature* **363**, 561–565 (1993).
- <sup>13</sup>S. Benabou, A. Aviñó, R. Eritja, C. González, and R. Gargallo, “Fundamental aspects of the nucleic acid i-motif structures,” *RSC Adv.* **4**, 26956–26980 (2014).
- <sup>14</sup>H. A. Day, C. Huguin, and Z. A. E. Waller, “Silver cations fold i-motif at neutral pH,” *Chem. Commun.* **49**, 7696–7698 (2013).
- <sup>15</sup>Y. Wang, H. Zhao, C. Yang, J. Jie, X. Dai, Q. Zhou, K. Liu, D. Song, and H. Su, “Degradation of cytosine radical cations in 2′-deoxycytidine and in i-motif DNA: Hydrogen-bonding guided pathways,” *J. Am. Chem. Soc.* **141**, 1970–1979 (2019).
- <sup>16</sup>B. Cohen, M. H. Larson, and B. Kohler, “Ultrafast excited-state dynamics of RNA and DNA C tracts,” *Chem. Phys.* **350**, 165–174 (2008).
- <sup>17</sup>P. M. Keane, M. Wojdyla, G. W. Doorley, J. M. Kelly, A. W. Parker, I. P. Clark, G. M. Greetham, M. Towrie, L. M. Magno, and S. J. Quinn, “Long-lived excited states in i-motif DNA studied by picosecond time-resolved IR spectroscopy,” *Chem. Commun.* **50**, 2990–2992 (2014).
- <sup>18</sup>P. M. Keane, F. R. Baptista, S. P. Gurung, S. J. Devereux, I. V. Sazanovich, M. Towrie, J. A. Brazier, C. J. Cardin, J. M. Kelly, and S. J. Quinn, “Long-lived excited-state dynamics of i-motif structures probed by time-resolved infrared spectroscopy,” *ChemPhysChem* **17**, 1281–1287 (2016).
- <sup>19</sup>Z. V. Reveguk, E. V. Khoroshilov, A. V. Sharkov, V. A. Pomogaev, A. A. Buglak, A. N. Tarnovsky, and A. I. Kononov, “Exciton absorption and luminescence in i-motif DNA,” *Sci. Rep.* **9**, 15988 (2019).
- <sup>20</sup>M. R. Carro Temboury, V. Paolucci, E. N. Hooley, L. Latterini, and T. Vösch, “Probing DNA-stabilized fluorescent silver nanocluster spectral heterogeneity by time-correlated single photon counting,” *Analyst* **141**, 123–130 (2016).
- <sup>21</sup>A. Terrón, B. Moreno-Vachiano, A. Bauzá, A. García-Raso, J. J. Fiol, M. Barceló-Oliver, E. Molins, and A. Frontera, “X-ray crystal structure of a metalated double-helix generated by infinite and consecutive C<sup>+</sup>-AgI-C<sup>+</sup> (C<sup>+</sup>:N1-hexylcytosine) base pairs through argentophilic and hydrogen bond interactions,” *Chem. - Eur. J.* **23**, 2103–2108 (2017).
- <sup>22</sup>H. Liu, F. Shen, P. Haruehanroengra, Q. Yao, Y. Cheng, Y. Chen, C. Yang, J. Zhang, B. Wu, Q. Luo, R. Cui, J. Li, J. Ma, J. Sheng, and J. Gan, “A DNA structure containing Ag-I-mediated G:G and C:C base pairs,” *Angew. Chem., Int. Ed.* **56**, 9430–9434 (2017).
- <sup>23</sup>D. J. E. Huard, A. Demissie, D. Kim, D. Lewis, R. M. Dickson, J. T. Petty, and R. L. Lieberman, “Atomic structure of a fluorescent Ag<sub>8</sub> cluster templated by a multistranded DNA scaffold,” *J. Am. Chem. Soc.* **141**, 11465–11470 (2019).
- <sup>24</sup>F. Linares, E. García-Fernández, F. J. López-Garzón, M. Domingo-García, A. Orte, A. Rodríguez-Diéguez, and M. A. Galindo, “Multifunctional behavior of molecules comprising stacked cytosine-Ag-I-cytosine base pairs; towards



- conducting and photoluminescence silver-DNA nanowires," *Chem. Sci.* **10**, 1126–1137 (2019).
- <sup>25</sup>J. Kondo, Y. Tada, T. Dairaku, Y. Hattori, H. Saneyoshi, A. Ono, and Y. Tanaka, "A metallo-DNA nanowire with uninterrupted one-dimensional silver array," *Nat. Chem.* **9**, 956–960 (2017).
- <sup>26</sup>J. Zhou, C. Wei, G. Jia, X. Wang, Z. Feng, and C. Li, "Formation of i-motif structure at neutral and slightly alkaline pH," *Mol. Biosyst.* **6**, 580–586 (2010).
- <sup>27</sup>M. Zeraati, D. B. Langley, P. Schofield, A. L. Moye, R. Rouet, W. E. Hughes, T. M. Bryan, M. E. Dinger, and D. Christ, "I-motif DNA structures are formed in the nuclei of human cells," *Nat. Chem.* **10**, 631–637 (2018).
- <sup>28</sup>S. M. Swasey, L. E. Leal, O. Lopez-Acevedo, J. Pavlovich, and E. G. Gwinn, "Silver(I) as DNA glue: Ag<sup>+</sup>-mediated guanine pairing revealed by removing Watson-Crick constraints," *Sci. Rep.* **5**, 10163 (2015).
- <sup>29</sup>S. M. Swasey and E. G. Gwinn, "Silver-mediated base pairings: Towards dynamic DNA nanostructures with enhanced chemical and thermal stability," *New J. Phys.* **18**, 045008 (2016).
- <sup>30</sup>Y. Dong, Z. Yang, and D. Liu, "DNA nanotechnology based on i-motif structures," *Acc. Chem. Res.* **47**, 1853–1860 (2014).
- <sup>31</sup>I. Goncharova, "Ag(I)-mediated homo and hetero pairs of guanosine and cytidine: Monitoring by circular dichroism spectroscopy," *Spectrochim. Acta, Part A* **118**, 221–227 (2014).
- <sup>32</sup>R. Lavery, K. Zakrzewska, J.-S. Sun, and S. C. Harvey, "A comprehensive classification of nucleic acid structural families based on strand direction and base pairing," *Nucleic Acids Res.* **20**, 5011–5016 (1992).
- <sup>33</sup>I. A. Rose, K. R. Hanson, K. D. Wilkinson, and M. J. Wimmer, "A suggestion for naming faces of ring compounds," *Proc. Natl. Acad. Sci. U. S. A.* **77**, 2439–2441 (1980).
- <sup>34</sup>C. R. Cantor, M. M. Warshaw, and H. Shapiro, "Oligonucleotide interactions. 3. Circular dichroism studies of the conformation of deoxyoligonucleotides," *Biopolymers* **9**, 1059–1077 (1970).
- <sup>35</sup>C. Grieco, J. M. Empey, F. R. Kohl, and B. Kohler, "Probing eumelanin photoprotection using a catechol:quinone heterodimer model system," *Faraday Discuss.* **216**, 520–537 (2019).
- <sup>36</sup>C. Grieco, F. R. Kohl, Y. Zhang, S. Natarajan, L. Blancafort, and B. Kohler, "Intermolecular hydrogen bonding modulates O–H photodissociation in molecular aggregates of a catechol derivative," *Photochem. Photobiol.* **95**, 163–175 (2019).
- <sup>37</sup>J. J. Snellenburg, S. P. Liptonok, R. Seger, K. M. Mullen, and I. H. M. van Stokkum, "Glotaran: A java-based graphical user interface for the R package TIMP," *J. Stat. Software* **49**, 1–22 (2012).
- <sup>38</sup>Y. Zhao, N. E. Schultz, and D. G. Truhlar, "Design of density functionals by combining the method of constraint satisfaction with parametrization for thermochemistry, thermochemical kinetics, and noncovalent interactions," *J. Chem. Theory Comput.* **2**, 364–382 (2006).
- <sup>39</sup>Y. Zhao and D. G. Truhlar, "Density functionals with broad applicability in chemistry," *Acc. Chem. Res.* **41**, 157–167 (2008).
- <sup>40</sup>D. Andrae, U. Häußermann, M. Dolg, H. Stoll, and H. Preuß, "Energy-adjusted *ab initio* pseudopotentials for the second and third row transition elements," *Theor. Chim. Acta* **77**, 123–141 (1990).
- <sup>41</sup>S. Miertuš, E. Scrocco, and J. Tomasi, "Electrostatic interaction of a solute with a continuum. A direct utilization of *ab initio* molecular potentials for the prevision of solvent effects," *Chem. Phys.* **55**, 117–129 (1981).
- <sup>42</sup>J. Tomasi, B. Mennucci, and R. Cammi, "Quantum mechanical continuum solvation models," *Chem. Rev.* **105**, 2999–3094 (2005).
- <sup>43</sup>M. Deiana, B. Mettra, L. Martinez-Fernandez, L. M. Mazur, K. Pawlik, C. Andraud, M. Samoc, R. Improta, C. Monnerau, and K. Matczyszyn, "Specific recognition of G-quadruplexes over duplex-DNA by a macromolecular NIR two-photon fluorescent probe," *J. Phys. Chem. Lett.* **8**, 5915–5920 (2017).
- <sup>44</sup>L. Martinez-Fernandez, T. Fahleson, P. Norman, F. Santoro, S. Coriani, and R. Improta, "Optical absorption and magnetic circular dichroism spectra of thioracils: A quantum mechanical study in solution," *Photochem. Photobiol. Sci.* **16**, 1415–1423 (2017).
- <sup>45</sup>M. Schmid, L. Martinez-Fernandez, D. Markovitsi, F. Santoro, F. Hache, R. Improta, and P. Changenet, "Unveiling excited-state Chirality of binaphthols by femtosecond circular dichroism and quantum chemical calculations," *J. Phys. Chem. Lett.* **10**, 4089–4094 (2019).
- <sup>46</sup>H. Herrmann, "On the photolysis of simple anions and neutral molecules as sources of O-/OH, SOx- and Cl in aqueous solution," *Phys. Chem. Chem. Phys.* **9**, 3935–3964 (2007).
- <sup>47</sup>A. I. S. Holm, L. M. Nielsen, B. Kohler, S. V. Hoffmann, and S. B. Nielsen, "Electronic coupling between cytosine bases in DNA single strands and i-motifs revealed from synchrotron radiation circular dichroism experiments," *Phys. Chem. Chem. Phys.* **12**, 3426–3430 (2010).
- <sup>48</sup>P. M. Keane, M. Wojdyla, G. W. Doorley, J. M. Kelly, I. P. Clark, A. W. Parker, G. M. Greetham, M. Towrie, L. M. Magno, and S. J. Quinn, "Ultrafast IR spectroscopy of polymeric cytosine nucleic acids reveal the long-lived species is due to a localised state," *Phys. Chem. Chem. Phys.* **14**, 6307–6311 (2012).
- <sup>49</sup>D. M. Gray and F. J. Bollum, "A circular dichroism study of poly dG, poly dC, and poly dG:dC," *Biopolymers* **13**, 2087–2102 (1974).
- <sup>50</sup>S. M. Swasey, N. Karimova, C. M. Aikens, D. E. Schultz, A. J. Simon, and E. G. Gwinn, "Chiral electronic transitions in fluorescent silver clusters stabilized by DNA," *ACS Nano* **8**, 6883–6892 (2014).
- <sup>51</sup>M. Berdakin, G. Féraud, C. Dedonder-Lardeux, C. Jouvet, and G. A. Pino, "Effect of Ag<sup>+</sup> on the excited-state properties of a gas-phase (Cytosine)<sub>2</sub>Ag<sup>+</sup> complex: Electronic transition and estimated lifetime," *J. Phys. Chem. Lett.* **5**, 2295–2301 (2014).
- <sup>52</sup>J. Müller, "Metal-mediated base pairs in parallel-stranded DNA," *Beilstein J. Org. Chem.* **13**, 2671–2681 (2017).
- <sup>53</sup>L. A. Espinosa Leal, A. Karpenko, S. Swasey, E. G. Gwinn, V. Rojas-Cervellera, C. Rovira, and O. Lopez-Acevedo, "The role of hydrogen bonds in the stabilization of silver-mediated cytosine tetramers," *J. Phys. Chem. Lett.* **6**, 4061–4066 (2015).
- <sup>54</sup>D. A. Megger and J. Müller, "Silver(I)-mediated cytosine self-pairing is preferred over Hoogsteen-type base pairs with the artificial nucleobase 1,3-dideaza-6-nitropurine," *Nucleosides, Nucleotides Nucleic Acids* **29**, 27–38 (2010).
- <sup>55</sup>S. M. Swasey, F. Rosu, S. M. Copp, V. Gabelica, and E. G. Gwinn, "Parallel guanine duplex and cytosine duplex DNA with uninterrupted spines of Ag-I-mediated base pairs," *J. Phys. Chem. Lett.* **9**, 6605–6610 (2018).
- <sup>56</sup>X. Chen, A. Karpenko, and O. Lopez-Acevedo, "Silver-mediated double helix: Structural parameters for a robust DNA building block," *ACS Omega* **2**, 7343–7348 (2017).
- <sup>57</sup>R. E. Dickerson, "Definitions and nomenclature of nucleic acid structure components," *Nucleic Acids Res.* **17**, 1797–1803 (1989).
- <sup>58</sup>M. A. El Hassan and C. R. Calladine, "Propeller-twisting of base-pairs and the conformational mobility of dinucleotide steps in DNA," *J. Mol. Biol.* **259**, 95–103 (1996).
- <sup>59</sup>C. Ma, C. C.-W. Cheng, C. T.-L. Chan, R. C.-T. Chan, and W.-M. Kwok, "Remarkable effects of solvent and substitution on the photo-dynamics of cytosine: A femtosecond broadband time-resolved fluorescence and transient absorption study," *Phys. Chem. Chem. Phys.* **17**, 19045–19057 (2015).
- <sup>60</sup>L. Martínez-Fernández, A. J. Pepino, J. Segarra-Martí, J. Jovaišaitė, I. Vaya, A. Nenov, D. Markovitsi, T. Gustavsson, A. Banyasz, M. Garavelli, and R. Improta, "Photophysics of deoxycytidine and 5-methyldeoxycytidine in solution: A comprehensive picture by quantum mechanical calculations and femtosecond fluorescence spectroscopy," *J. Am. Chem. Soc.* **139**, 7780–7791 (2017).
- <sup>61</sup>C. Ma, R. C.-T. Chan, C. T.-L. Chan, A. K.-W. Wong, B. P.-Y. Chung, and W.-M. Kwok, "Fluorescence and ultrafast fluorescence unveil the formation, folding molecularly, and excitation dynamics of homo-oligomeric and human telomeric i-motifs at acidic and neutral pH," *Chem. - Asian J.* **13**, 3706–3717 (2018).
- <sup>62</sup>C. A. Schroeder, E. Pluhařová, R. Seidel, W. P. Schroeder, M. Faubel, P. Slavíček, B. Winter, P. Jungwirth, and S. E. Bradforth, "Oxidation half-reaction of aqueous nucleosides and nucleotides via photoelectron spectroscopy augmented by *ab initio* calculations," *J. Am. Chem. Soc.* **137**, 201–209 (2015).
- <sup>63</sup>M. I. Taccone, G. Féraud, M. Berdakin, C. Dedonder-Lardeux, C. Jouvet, and G. A. Pino, "Communication: UV photoionization of cytosine catalyzed by Ag<sup>+</sup>," *J. Chem. Phys.* **143**, 041103 (2015).
- <sup>64</sup>A. Terrón, L. Tomàs, A. Bauzá, A. García-Raso, J. J. Fiol, E. Molins, and A. Frontera, "The first X-ray structure of a silver-nucleotide complex: Interaction



of ion Ag(I) with cytidine-5'-monophosphate," *CrystEngComm* **19**, 5830–5834 (2017).

<sup>65</sup>B. Sharma, A. Mahata, S. Mandani, T. K. Sarma, and B. Pathak, "Coordination polymer hydrogels through Ag(I)-mediated spontaneous self-assembly of unsubstituted nucleobases and their antimicrobial activity," *RSC Adv.* **6**, 62968–62973 (2016).

<sup>66</sup>L. Mistry, P. G. Waddell, N. G. Wright, B. R. Horrocks, and A. Houlton, "Transoid and cisoid conformations in silver-mediated cytosine base pairs: Hydrogen bonding dictates argentophilic interactions in the solid state," *Inorg. Chem.* **58**, 13346–13352 (2019).

<sup>67</sup>J. Ma, F. Wang, S. A. Denisov, A. Adhikary, and M. Mostafavi, "Reactivity of prehydrated electrons toward nucleobases and nucleotides in aqueous solution," *Sci. Adv.* **3**, e1701669 (2017).

<sup>68</sup>I. G. Gut, P. D. Wood, and R. W. Redmond, "Interaction of triplet photosensitizers with nucleotides and DNA in aqueous solution at room temperature," *J. Am. Chem. Soc.* **118**, 2366–2373 (1996).

<sup>69</sup>D. J. Gibbons, A. Farawar, P. Mazzella, S. Leroy-Lhez, and R. M. Williams, "Making triplets from photo-generated charges: Observations, mechanisms and theory," *Photochem. Photobiol. Sci.* **19**, 136–158 (2020).